

# STUDY ON BUCKLING BEHAVIOUR OF LAMINATED SHELLS UNDER PULSE LOADING

E. Eglitis\*, K.Kalnins\*, C. Bisagni\*\*

\*Riga Technical University, Institute of Materials and Structures, Latvia,

\*\*Politecnico di Milano, Dipartimento di Ingegneria Aerospaziale, Italy

**Keywords:** *dynamic buckling, buckling tests, pulse loads, composite shells, imperfections*

## Abstract

*This experimental and numerical study focuses on the buckling problem of cylindrical composite shells under pulse loads. Series of experiments have been performed to determine buckling loads of the laminated cylinders under different axial loading rates. Numerical models of the tested specimens have been elaborated and good agreement between experimental and numerical results has been achieved. The numerical models have been used to study the buckling behavior of the cylinders at loading rates much higher than could be achieved experimentally. Additionally, the influence of imperfections on dynamic buckling behavior of the laminated shells has been studied numerically.*

## 1 Introduction

Laminated composites are widely used in design of lightweight structures, where minimization of the weight is essential, e.g., in transportation industry, especially aviation. Within these applications, the highest loads that drive the design of a structural component may have very short durations, and therefore dynamic buckling should be considered.

As the thin-walled structures tend to fully exploit the strength and stiffness of material, special attention has to be paid to maintain the reliability. Assuming the loading as quasi-static can lead to over-designed structures on one hand, as the buckling load can increase when the load has short durations [1-3]. On the other hand, when loading frequency is close to the lowest natural frequency of the structure, or the load is applied suddenly, investigations show

that buckling strength can be significantly less than under static loading [1, 4-7]. Therefore, it is fundamental to improve both efficiency and reliability of the design, considering the load as dynamic and understanding its effect on the load carrying capacity of the structure.

Even though dynamic effects on buckling of shells are of importance, there are very few experimental studies in this field. Some experimental results on dynamic buckling of columns and plates are presented by Ari-Gur et al. [8], Weller et al. [9], Abramovich and Grunwald [6] and Cui et al. [10, 11]. Among the first authors to investigate dynamic buckling of thin cylindrical shells experimentally are Koval and Oneill [12] and Humphereys and Sve [13] in the sixties.

Zimick and Tennyson presented their experimental results on thin-walled circular cylindrical shells subjected to dynamic, transient, axial square-wave loading of varying time duration [14]. The results indicate that buckling stiffness increased dramatically for short durations of loading due to the shell inertia in the radial direction. For short time durations the dynamic buckling stress was increased above static for even relatively imperfect models. Because of the good agreement obtained between experiment and analysis, it is concluded that the simplified analytical buckling model used in the study adequately accounts for the principal mechanisms governing the dynamic response of circular cylinders.

Yaffe and Abramovich investigated buckling of aluminum cylindrical stringer stiffened shells under axial dynamic applied loading, both numerically and experimentally [1]. The authors conclude that even though the

simple test set-up worked properly and the dynamic buckling of the shell was observed, no test results were obtained to form a sound experimental database for this phenomenon.

Imperfection sensitivity of the axially compressed cylindrical shells is widely acknowledged and cannot be neglected in a shell buckling study. The imperfection sensitivity of cylinders has been studied analytically by several investigators, such as Bolotin [14], Faser and Budiansky [15] and Amazigo [16]. Singer and Abramovich reviewed the development of imperfection measurement techniques since sixties until mid-nineties [17]. It is outlined that until late sixties only partial imperfection measurements have been made and out-of-roundness criterion was established as a measure of imperfection of the shell. Only in the late seventies the measurements of geometric imperfections became an integral part of a properly carried out shell buckling test, and majority of numerical studies also consider the imperfections measured on real specimens [4, 18]

The present investigation focuses on the effect of loading rate and duration on buckling behavior of thin axially compressed laminated composite shells. Several cylindrical specimens have been produced of glass fiber fabric reinforced plastic for the experimental part of the investigation.

## 2 Specimens

Fifteen cylindrical specimens have been produced of glass fiber fabric reinforced plastic (GFRP) for the experimental part of the investigation. The specimens have diameters  $D$  of 300 and 500 mm and lengths  $L$  varying from 400 to 660 mm. The nominal wall thickness for all specimens is 1.1 mm, and the specimens are designed to withstand repeated buckling deformations. The dimensions of each specimen and their designations are presented in Table 1.

Each specimen is composed of four layers of 290 g/m<sup>2</sup> E-glass fiber fabric and Polylyte 440 polyester resin, manually applied to a cylindrical mandrel and arranged in sequence  $[0_F]_4$ . Vacuum resin impregnation has been used to achieve consistent material properties.

Table 1. Dimensions of specimens

		Diameter $D$		
		300 mm	500 mm	
Free length $L$	400 mm	400-1	-	
		400-2		
		400-3		
		400-4		
	560 mm	560-1	-	
		560-2		
		560-3		
		560-4		
	660 mm	-	660-1	660-5
			660-2	660-6
			660-3	660-7
			660-4	

Flat coupons have been produced using the same fibers, resin and vacuum impregnation technology for identification of material mechanical properties according to ISO 527-4:2000 [19] standard. The identified material properties are presented in Table 2.

The ends of the specimens are encasted in flat plates using epoxy resin with aluminum powder as aggregate to ensure consistent boundary conditions and even load distribution (Fig. 1).

## 3 Experimental Set-up

The experimental rig prepared at the laboratory of the RTU Institute of Materials and Structures is based on Inston 8802 hydraulic frame. The



Fig. 1. Specimen 660-4

load is being introduced by the hydraulic actuator of 250 kN capacity located at the top of the frame (Fig. 2) and transferred to the specimen through a grip and a steel loading plate. The specimen is supported by another steel plate, which is placed on a spherical bearing. The bearing is attached to the lower grip, and its rotation centre is located 150 mm above the bottom plate. The load cell that registers the axial load of the cylinder is located below the lower grip, on the bottom of the frame.

This experimental rig allows performing static buckling tests, as well as dynamic buckling tests with loading rate of 170 mm/s.

In order to monitor the post-buckling shapes of the cylinders during the static buckling tests, a basic interferometry set-up has been created. A moiré fringe with both line thickness and distance between lines of 1 mm was placed in front of the specimens. Placing a spotlight and a camera at different angles resulted in pictures with moiré patterns clearly indicating buckling shapes on the pictures (Fig. 5).

Table 2. Properties of GFRP

Property	Direction	Value
Tensile modulus (GPa)	$E_1$	18.66
	$E_2$	18.28
Poisson's ratio	$\nu_{12}$	0.16
Shear modulus (GPa)	$G_{12}$	4.56
Tensile strength (MPa)	$\sigma_1$	219
	$\sigma_2$	296

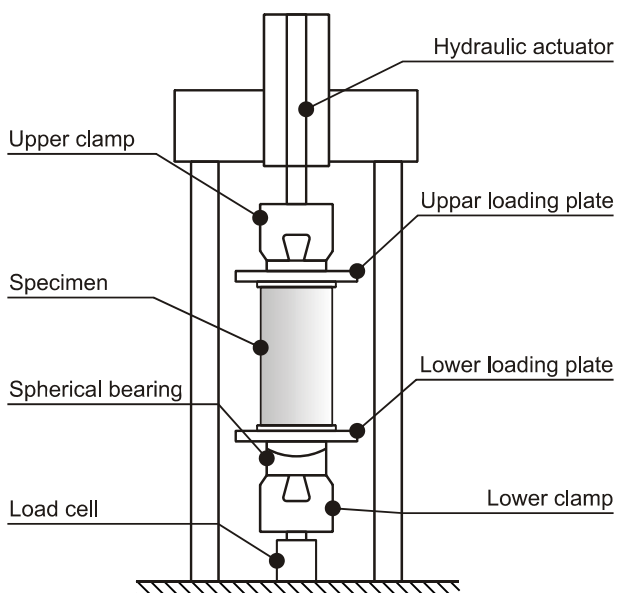


Fig. 2. Buckling test set-up

All the tests in this study were displacement – controlled.

## 4 Experimental Results

Buckling tests have been performed repeatedly on all specimens. First, the static buckling tests have been performed, and the load-shortening curves and post-buckling shapes recorded.

One specimen from each configuration with the most consistent static buckling results has been chosen for dynamic pulse buckling tests.

### 4.1 Static buckling tests

All the specimens were repeatedly loaded until post-buckling to determine the buckling loads and corresponding buckling shapes within a timeframe of 6 months. Load-shortening curves have been recorded, and pictures of buckling shapes taken.

The scatters of obtained critical load values for specimens with diameters of 300 mm and 500 mm are summarized in Figure 3 and Figure 4, respectively. The typical obtained buckling shapes are presented in Figure 5.

It must be noted, that the scatter of the static buckling loads for each specimen configuration is significant: for specimens with  $L = 400$  mm the standard deviation is 7.7%, and for specimens with  $L = 560$  mm and  $L = 660$  mm it is 9.8% and 13.6%, respectively.

It is also evident that the specimens that have the buckling shape close to the ‘diamond shape’ usually have higher and more consistent buckling loads.

Considering the scatter of the static buckling loads, the specimens chosen from each configuration for the dynamic buckling tests are 400-4, 560-2 and 660-4.

### 4.2 Dynamic buckling tests

The dynamic buckling tests have been performed under displacement control, using a triangular load pulse. This loading history has been chosen because of the limited maximum velocity and acceleration of the hydraulic actuator on one hand, and need to stop the

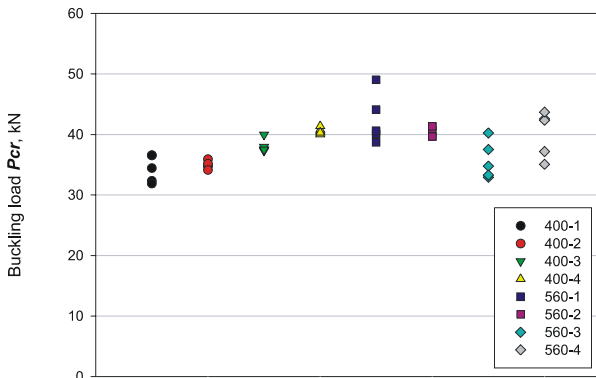


Fig. 3. Static buckling loads for specimens  $D=300\text{mm}$

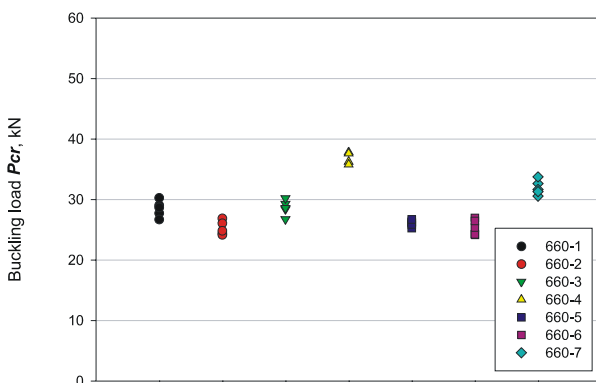


Fig. 4. Static buckling loads for specimens  $D=500\text{mm}$

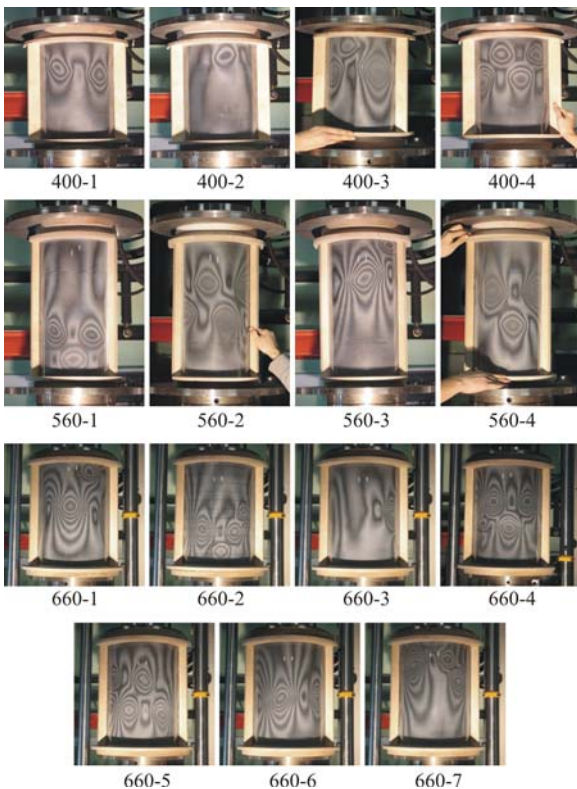


Fig. 5. Static buckling shapes

actuator after the buckling to keep the specimen undamaged on the other hand. The use of the triangular pulse allowed maximizing the loading rate at the moment of buckling and also is somewhat similar to the loading history used in the numerical study. Along with the maximum loading rate of 170 mm/s, loading rates of 140 mm/s, 70 mm/s and 40 mm/s were used. Sample displacement-time histories are presented in Figure 6.

Since the dynamic loading rates were relatively low, the maximum loads registered are considered critical in the experimental study. The load-shortening curves for each of the considered specimens are presented in Figure 7, and the buckling loads at different loading histories and corresponding Dynamic Load Factors (DLF) are summarized in Table 3.

The general tendency of increase in DLF along with increase of loading velocity is evident. However, due to the limited maximum loading velocity, additional numerical studies have to be performed.

### 5 Numerical Modeling

ABAQUS/Explicit [20] finite element code has been used to carry out numerical simulations of the buckling experiments performed within this study. Additionally, ABAQUS/Implicit has been used for linear buckling and natural frequency analyses. The loading rate of 10 mm/s has been chosen for the simulations of quasi-static tests.

The S4R four node shell elements have been employed and, according to the results of

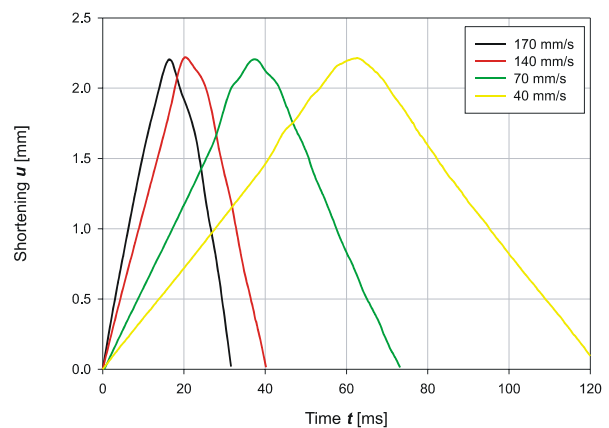


Fig. 6. Shortening-time curves for specimen 560-2

Table 3. Experimental dynamic buckling test results

Loading velocity	Spec. 400-4		Spec. 560-2		Spec. 660-4	
	$P_{cr}$ , kN	DLF	$P_{cr}$ , kN	DLF	$P_{cr}$ , kN	DLF
Quasistatic	41.69	1.00	40.60	1.00	36.24	1.00
40 mm/s	45.23	1.08	42.68	1.05	42.68	1.18
70 mm/s	46.74	1.12	45.09	1.11	44.31	1.22
140 mm/s	48.21	1.16	47.56	1.17	45.56	1.26
170 mm/s	47.51	1.14	48.53	1.20	46.37	1.28

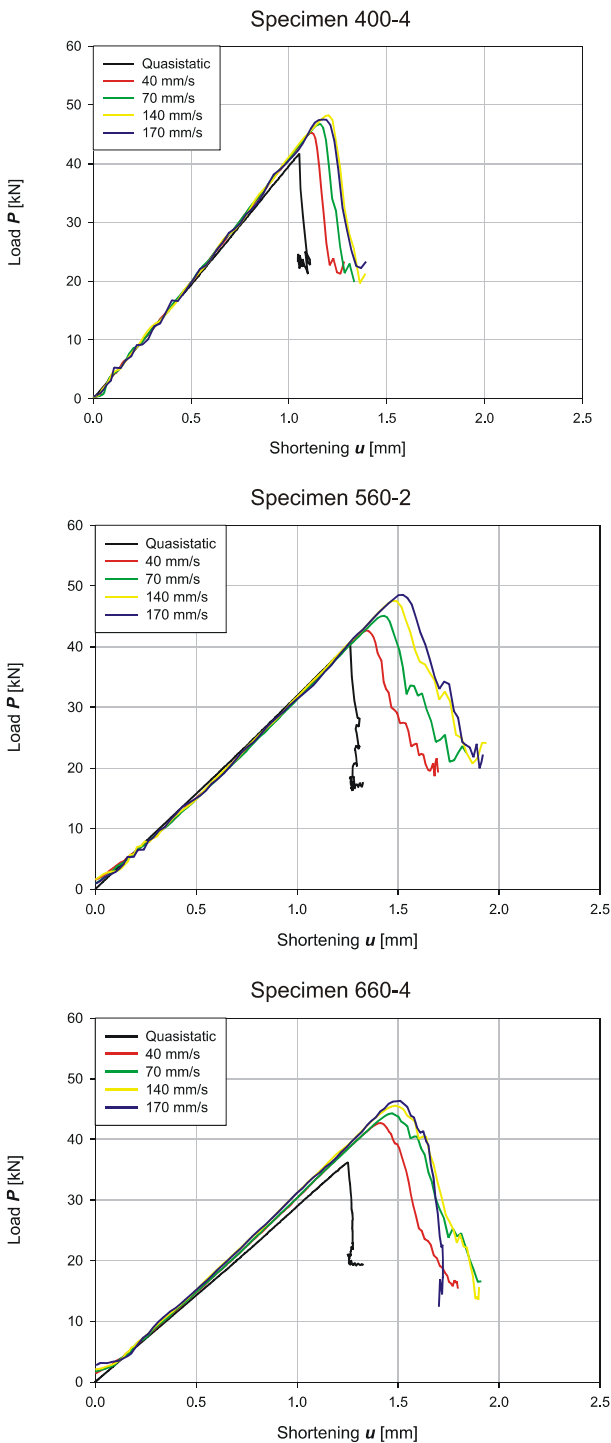


Fig. 7. Load-shortening curves of dynamic buckling tests

the mesh sensitivity analysis, the nominal dimension of an element was chosen to be  $1/20$  of the shell radius  $R$ .

The spherical bearing, which is present in the experimental set-up, has been modeled as a set of rigid elements that connects the master node located at the center of rotation of the bearing with the lower edge of the specimen. All the translations are constrained for this master node, but all the rotations are allowed. The only degree of freedom allowed at the upper edge is translation in axial direction, where the load is introduced.

### 5.1 Imperfection influence and benchmarking of numerical models

The imperfection sensitivity of axially compressed cylindrical shells is widely accepted and imperfection measurements of shells are a significant part of buckling test procedure [4, 17, 18, 21]. However, the actual imperfections of the specimens under investigation could not be measured, therefore imperfection influence on dynamic buckling behavior has been studied numerically using three different imperfection shapes:

- First eigenmode of eigenvalue buckling analysis performed on the model ('checkboard' pattern, Figure 8 a)
- First eigenmode of eigenvalue buckling analysis, performed on the model with isotropic material properties (axisymmetric pattern, Figure 8 b)
- Imperfections measured at Politecnico di Milano on other specimens, produced using the same technology and mandrel (realistic pattern, Figure 8 c)

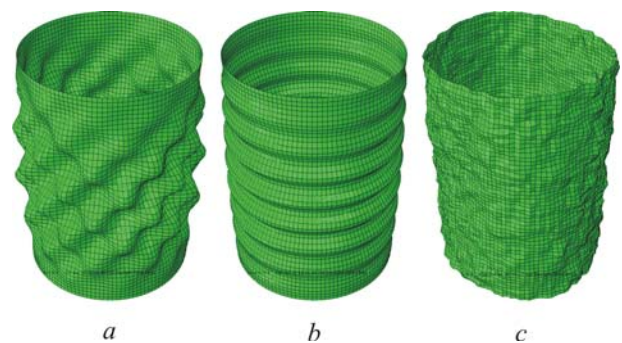


Fig. 8. Imperfection patterns (not to scale)

The numerical models have been updated with each of the imperfection shapes considered and the experimental shortening-time histories have been simulated using ABAQUS/Explicit. Some of the obtained load-shortening curves for the model of specimen 560-2 are presented in Figure 9. For each specimen, the imperfection shape that resulted in the best correlation with

the experimental data (e.g. axisymmetric pattern for specimen 560-2, in Fig. 9) is considered to be the best representation of actual imperfections and used further in this study. It can be seen from Fig. 9 that dynamic buckling phenomenon is also imperfection sensitive, and for the same shortening-time histories the DLFs are dependent on the initial imperfection shape.

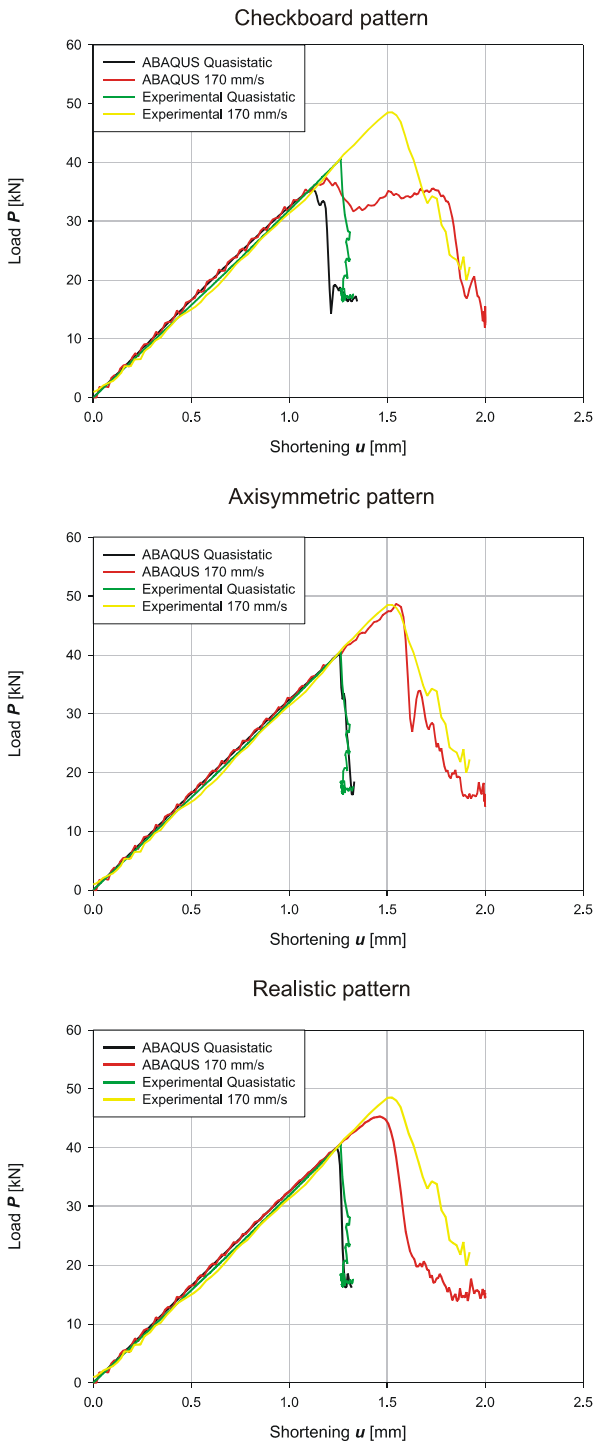


Fig. 9. Influence of imperfections

## 6 Numerical Results

Series of simulations have been carried out to construct a dynamic buckling load versus load duration plots for each specimen configuration. The loading rates were ranging from 1 kN/ms to 960 kN/ms, covering the range from 0.26 ms to 43 ms.

For shorter loading durations it is difficult to determine the critical load for a displacement-controlled simulation. Therefore, to study the dependency of DLF on the loading rate, the load has been applied at given rates, and the out-of-plane displacements have been monitored. From these data, a Budiansky-Hutchinson plot [22] is constructed for each simulation, and the load is considered critical when the maximum out-of-plane displacement of a node reaches 1 mm. This tolerance has been selected to exclude oscillations caused by dynamic loading. Example of these plots for specimen 560-2 and different loading rates are presented in Figure 10.

### 6.1 Natural frequencies

In their study on dynamic buckling of cylindrical stringer stiffened shells [1], Yaffe and Abramovich expected to obtain  $DLF < 1$  with load pulse duration of equal to half of longest natural bending period  $\tau$ , similarly as in cases of columns and plates. However, their numerical results showed that the DLF could drop below unity, when loading period  $T = 2a/c$ , where  $a$  is the length of the cylinder and  $c$  is the speed of sound in the shell.

To make sure the study covers these critical areas, natural bending periods have been calculated using ABAQUS/Standard and speed of sound in the shell evaluated. The load durations that could lead to  $DLF < 1$  are summarized in Table 4.

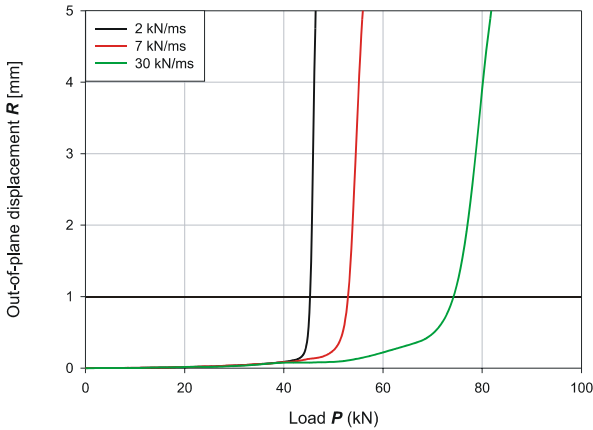


Fig. 10. Budiansky-Hutchinson plot

### 6.2 Influence of load duration

The dependency of the dynamic buckling load on the load duration is presented in Figure 11.

At lowest loading rates considered, buckling modes are similar to the static buckling mode, but with larger number of longitudinal waves (Figure 12 a). When the load duration approaches the critical  $T = \tau/2$ , the buckling mode starts to transform to an axisymmetric mode (Figure 12 b). Further increase of the loading rate and decrease of the load duration leads to axisymmetric buckling mode (Figure 13 c), and a slight drop of DLF can be observed when the load duration is close to  $T = 2a/c$ .

Table 4. Natural periods of specimens

Model	$T = \tau/2$ [ms]	$T = 2a/c$ [ms]
400-4	1.46	0.31
560-2	2.02	0.43
660-4	3.03	0.51

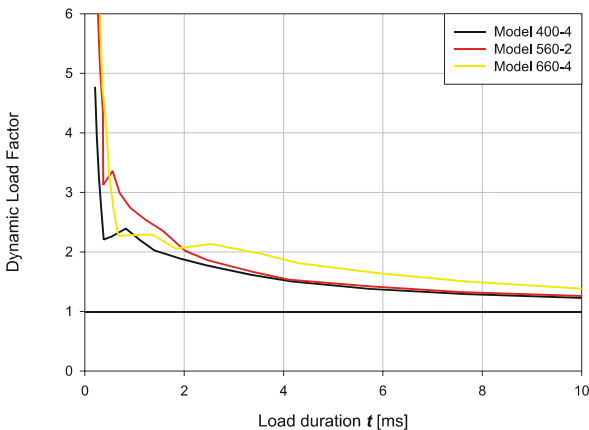


Fig. 11 DLF versus load duration

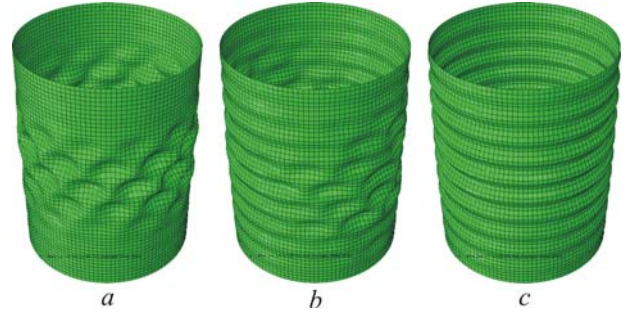


Fig. 12 Dynamic buckling shapes (not to scale)

## 7 Conclusions

Dynamic pulse buckling of axially compressed composite cylindrical shells has been studied experimentally and numerically.

Static and dynamic buckling tests have been performed on E-glass fiber reinforced cylinders to evaluate the effect of loading velocity on buckling loads. The velocities of displacement-controlled dynamic loading have been in range from 40 to 170 mm/s, resulting in loading rates of 1.26 to 5.00 kN/ms. During the tests, there was a consistent increase of the buckling load with the increase of loading rate, resulting in all DLFs being greater than 1.

The experimental investigation was supported by numerical studies using ABAQUS finite element code. Models of the tested specimens have been created and influence of imperfections and loading rates on the buckling behavior has been studied. Depending on the shape of initial imperfections, DLFs from 1.06 to 1.19 have been achieved while keeping all the other conditions the same. It has been demonstrated that with successful choice of artificial initial imperfections, the numerical simulations of the experiments show good agreement in both cases of static and dynamic loading.

The buckling of the cylinders has been studied numerically at loading rates from 1 kN/ms to 960 kN/ms, which could not be achieved by the experimental equipment used. The results show almost consistent increase of the DLF across the studied range. This is somewhat contradicting the findings of other researchers, however, it must be noted that the load has been applied gradually until buckling in this study, unlike other studies, where the

loads are applied suddenly or half-sine shaped load-time histories are used.

This draws to the general conclusion that the laminated composite shell structures, which are loaded rapidly, yet gradually, can have the  $DLF > 1$  across all the dynamic loading range.

### Acknowledgement

This work has been partly supported by Latvian Council of Sciences through grants 09.1262 and 08.2132 and by the European Social Fund within the project "Support for the implementation of doctoral studies at Riga Technical University"

### References

- [1] Yaffe R, Abramovich H. Dynamic buckling of cylindrical stringer stiffened shells. *Composite Structures*, Vol. 81, pp 1031-1039, 2003
- [2] Zimick D.G, Tennyson R.C. Stability of circular cylindrical shells under transient axial impulsive loading. *AIAA Journal*, Vol. 18, pp 691-699, 1980
- [3] Pegg N.G. A numerical study of dynamic pulse buckling of cylindrical structures. *Marine Structures*, Vol. 7, pp 189-212, 1994
- [4] Bisagni C. Dynamic buckling of fiber composite shells under impulsive axial compression. *Thin-Walled Structures*, Vol. 43, pp 499-514, 2005
- [5] Lindberg H.E, Florence A.L. *Dynamic pulse buckling: theory and experiment*. 1st edition, Martinus Nijhoff publishers, 1987
- [6] Abramovich H., Grunwald A. Stability of axially impacted composite plates. *Composite Structures*, Vol. 32, pp 151-158, 1995
- [7] Huyan X, Simites G.J. Dynamic buckling of imperfect cylindrical shells under axial compression and bending moment. *AIAA Journal*, Vol. 35, pp 1404-1412, 1997
- [8] Ari-Gur J, Weller T, Singer J. Experimental and theoretical studies of columns under axial impact. *Int. J. of Solids and Structures*, Vol. 18, pp 619-641, 1982
- [9] Weller T, Abramovich H, Yaffe R. Dynamic buckling of beams and plates subjected to axial impact. *Computers and Structures*, Vol. 32, pp 835-851, 1989
- [10] Cui S, Cheong H.K, Hao H. Experimental study of dynamic post-buckling characteristics of columns under fluid-solid slamming. *Engineering Structures*, Vol. 22, pp 647-656, 2000
- [11] Cui S, Cheong H.K, Hao H. Experimental study of dynamic buckling of plates under fluid-solid slamming. *Int. J. of Impact Engineering*, Vol. 22, pp 675-691, 1999
- [12] Koval L.R, Oneill J.P. Structural responses to dynamic loading. *Proc AIAA annual meeting*, Washington, D.C., Vol. 1, paper 64-485, 18 p, 1964
- [13] Humphreys J.S, Sve C. Dynamic buckling of cylinders under axial shock-tube loading. *Proc AIAA annual meeting*, New York, N.Y., Vol. 3, paper 66-82, 11 p, 1966
- [14] Bolotin V.V. Statistical methods in the nonlinear theory of shells. *NASA TT F-85* (Translation of a paper presented at a seminar in the Institute of Mechanics of the Academy of Sciences of the USSR, 1957), 1962
- [15] Faser W.B., Budiansky B. The buckling of a column with random initial deflections. *Journal of Applied Mechanics*, Vol. 36, pp 233-240, 1969
- [16] Amazigo J. C. Buckling under axial compression of long cylindrical shells with random axisymmetric imperfections. *Quarterly of Applied Mathematics*, Vol. 26, pp 537-566, 1969
- [17] Singer J, Abramovich H. The development of shell imperfection measurement techniques. *Thin-Walled Structures*, Vol. 23, pp 379-398, 1995
- [18] Hilburger M.W, Starnes J.H. Effects of imperfections of the buckling response of composite shells. *Thin-Walled Structures*, Vol. 42, pp 369-397, 2004
- [19] ISO 527-4:1997 *Plastics - Determination of tensile properties - Part 4: Test conditions for isotropic and orthotropic fibre-reinforced plastic composites*. International Organization for Standardization, 1997
- [20] *ABAQUS Online Documentation: Version 6.8*, Dassault Systèmes, 2008
- [21] Eglitis E, Kalnins K, Ozolins O. The influence of loading eccentricity on buckling of axially compressed imperfect composite cylinders. *Mechanics of Composite Materials*, Vol. 46, 2010 (in press)
- [22] Budiansky B, Hutchinson J.W. Dynamic buckling of imperfection sensitive structures. *Proc International Congress of Applied Mechanics*, Munich, Germany, Vol. 11, pp 637-651, 1964

### Copyright Statement

The authors confirm that they, and/or their company or organization, hold copyright on all of the original material included in this paper. The authors also confirm that they have obtained permission, from the copyright holder of any third party material included in this paper, to publish it as part of their paper. The authors confirm that they give permission, or have obtained permission from the copyright holder of this paper, for the publication and distribution of this paper as part of the ICAS2010 proceedings or as individual off-prints from the proceedings.